

DISCRETE-TIME QUEUEING ANALYSIS OF POWER-SAVING MECHANISMS IN LTE DRX SYSTEMS WITH DIFFERENTIATED VACATION AND DISASTER

A MOHAMMED SHAPIQUE¹, A VAITHIYANATHAN²

^{1,2}IFET College of Engineering, Villupuram, India
shapique@gmail.com, vaithi05@gmail.com

Abstract

This paper investigates the power-saving mechanisms of Discontinuous Reception (DRX), a technique used in wireless communication networks to reduce energy consumption. By employing a discrete-time Geo/Geo/1 queueing model with differentiated vacations and system disasters, we aim to more accurately capture the intermittent nature of data arrivals, often overlooked in continuous-time models. Our research addresses the existing gap in the literature by providing a more realistic representation of DRX behaviour. Understanding the performance and characteristics of DRX is crucial for optimizing energy efficiency and improving the overall performance of wireless networks. This paper contributes to this understanding by deriving steady-state probabilities, calculating key performance metrics, and visualizing the system behaviour through graphical analysis.

Keywords: Geo/Geo/1, Differentiated vacation, Disaster, Repair, Generating function, Steady-state probabilities

1. INTRODUCTION

Queueing theory is a mathematical framework used to analyse systems where customers or jobs wait in line for service. It is essential in healthcare, manufacturing, communication, Internet of Things (IoT) and computer systems. For example, in a communication network, queueing theory helps predict data packet delays and optimise network performance. Network engineers can design more efficient and reliable systems by understanding the dynamics of queues. The proliferation of wireless devices and the increasing demand for seamless connectivity have created a critical need for energy-efficient communication systems. Power-Saving Mechanisms (PSMs) have emerged as a pivotal solution to address this challenge. Recently, queueing theory with vacations has emerged as a powerful tool for analysing PSM in wireless sensor networks [14], Internet of things [10] and wireless communication systems [12, 7]. By modelling the system as a queue where the server (e.g., a processor or network node) takes periodic vacations (e.g., entering a low-power state), queueing theory can provide valuable insights into the trade-offs between energy consumption and system performance. The paper aims to analyse the functions of Discontinuous Reception (DRX), a PSM applied in communication systems using the Geo/Geo/1 queueing model with differentiated vacation and system disaster.

Wireless devices are usually battery-powered, and their battery life significantly influences user experience [1]. Despite recent improvements in battery capacity, many users still complain about the limited battery life of their devices. Consequently, substantial research is focused on mitigating this issue. While one approach involves improving battery efficiency, increasing attention is given to incorporating energy-saving techniques within communication protocols. To

address energy efficiency concerns, the 3rd Generation Partnership Project (3GPP) introduced Discontinuous Reception (DRX) [21] as a mechanism to reduce energy consumption in wireless devices, referred to as User Equipment (UE) in 3GPP standards. The DRX mechanism is designed to extend the battery life of UEs by alternating between active and sleep modes while maintaining essential network connectivity.

The primary goal of DRX is to minimize power consumption when no data transmission occurs, primarily by allowing the UE's radio receiver to enter sleep mode for extended periods. In LTE DRX, there are three key states: Inactivity (Idle), Active, and Sleep periods, which are further divided into Short Sleep and Long Sleep periods. The Inactive and active periods represent power-active modes, while the Short and Long Sleep periods are power-saving modes. The functions of various modes of DRX are as follows:

- **Inactivity Period:** During this period, the DRX Inactivity Timer is active, and the UE monitors the Physical Downlink Control Channel (PDCCH) for potential downlink transmissions. If a transmission is detected, the UE switches to Active mode. The Short Sleep period begins if the Inactivity Timer expires without any transmission.
- **Short Sleep Period:** The DRX Short Cycle Timer is activated in this phase. The UE periodically wakes up to monitor the PDCCH. If a downlink transmission is detected, the UE transitions back to Active mode and restarts the Inactivity Timer. If no transmission is detected, the UE returns to Short Sleep until the Short Cycle Timer expires.
- **Long Sleep Period:** Once the Short Cycle Timer expires, the UE enters a deeper power-saving state called the Long Sleep period. Similar to the Short Sleep phase, the UE periodically wakes up to monitor the PDCCH but remains in Long Sleep until a transmission is detected or other network triggers occur.

This paper focuses on downlink transmissions, where the UE transitions between sleep and active states based on the status of the DRX Inactivity Timer. Several analytical studies have investigated the performance of DRX using vacation queuing models. Yang and Lin [19] proposed a Markov chain model to evaluate the DRX performance in UMTS systems, assuming downlink packet arrivals follow a Poisson process. Yang et al. [20] applied a semi-Markov process to analyze the PSM of DRX. Turck et al. [4] analyzed the PSM of WiMAX and DRX using a discrete-time queuing model. Recently, numerous authors have examined the PSM of DRX using the Differentiated Vacation (DV) policy introduced by Ibe and Isijola [5]. Unlike the classical multiple vacation queuing model, where the server embarks on another vacation of the same duration if no customers are present at the end of a vacation, the DV model is characterized by varying durations for subsequent vacations. The DV model operates with three states: busy, type-I vacation (T_{V_1}), and type-II vacation (T_{V_2}). After a busy period, the server enters T_{V_1} if no customers are waiting. If the system remains empty at the end of the T_{V_1} period, the server transitions to a T_{V_2} .

The DV policy has been analysed in various contexts. Ibe and Isijola [5] employed the DV policy to study human behaviour. Vijayashree and Janani [18] explored time-dependent probabilities in an M/M/1/DV queuing model. Sampath and Liu [13] introduced the concept of customer impatience into the M/M/1/DV model, presenting both transient and steady-state analyses. Kumar et al. [8] discussed a congestion model incorporating the DV policy and customer impatience. More recently, Shapique et al. [11] applied the M/M/1/DV queuing model to examine the PSM in WiMAX.

Disaster in a queuing system can be considered server failures [2], which can severely disrupt the functioning of the systems. Integrating these events into queuing models allows us to evaluate system robustness, analyse performance under adverse conditions, and formulate effective risk management strategies. Network outages, power failures, and electromagnetic interference can critically affect essential infrastructure and emergency response mechanisms in communication systems. Many authors analysed queuing systems with disaster [6, 9, 15]. Recently, continuous-time queuing systems with DV policy and system Disaster captured the

interest of several authors. Dimitriou [3] applied the M/G/1 queueing model to analyse the PSM of DRX with fault-tolerant. Sudhesh et al. [16] applied an M/M/1/DV queueing system with system disaster to analyse the PSM of DRX.

The existing literature shows that many studies have focused on continuous-time models to analyse the PSMs of DRX, providing valuable insights into performance under various conditions. However, the discrete nature of data transmission in wireless communication systems requires a more detailed and granular analysis. This paper addresses this gap by examining DRX functions within a discrete-time framework, explicitly using a Geo/Geo/1 queueing model with differentiated vacations. By adopting this discrete-time approach, the analysis more accurately captures the intermittent nature of data arrivals and the discrete-time operations intrinsic to DRX, leading to a more precise evaluation of system behaviour.

The structure of the paper is as follows: Section 2 presents the model description. Section 3 discusses the steady-state analysis of various states. Section 4 presents various performance indices of the proposed model. Section 5 deals with a numerical illustration of the model. Finally, Section 6 presents the conclusion of the work.

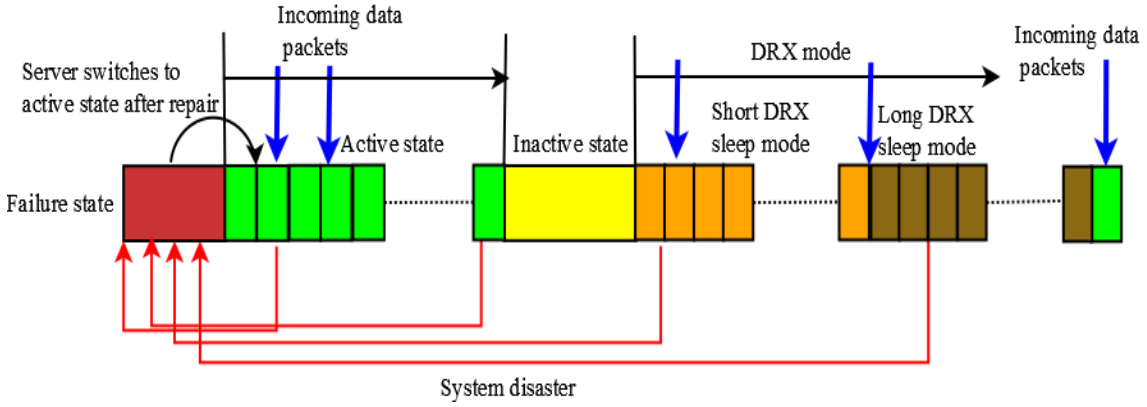


Figure 1: Pictorial representation of the investigated model

2. MODEL DESCRIPTION

This section presents the model description of a Geo/Geo/1 queueing system with a DV policy, where the system is subject to disaster and repair mechanisms. Data packets join the buffer with parameter λ , and the server provides service to these packets with rate μ . After serving all data packets, the server enters an idle state. If no new packets arrive within a specified idle timer Ψ , the server transitions to a T_{V_1} state, activating a timer κ_1 . If no packets are waiting at the end of the T_{V_1} timer κ_1 , the server transitions to a T_{V_2} state with rate θ , activating a timer κ_2 . Additionally, the system is subject to disasters that can occur at any state with rate ζ . When a disaster occurs, all packets in the system are lost, and the server enters a failure state. After repairs, which occur with rate ω , the server returns to the idle state. The system operates under a first-come, first-served service discipline. The detailed assumptions of the model are given below.

1. The data packets arrivals occur at the slot $t = n^-$, $n = 0, 1, 2$ and inter-arrival time τ follows a geometric distribution whose probability mass function is given by

$$P(\tau = n) = \lambda \bar{\lambda}^{n-1}, n = Z^+; \lambda \in (0, 1)$$

2. The probability mass function of service distribution is given by

$$P(S = n) = \mu \bar{\mu}^{n-1}, n = Z^+; \mu \in (0, 1)$$

3. The probability mass function of T_{V_1} and T_{V_2} is given by

$$P(V_i = n) = \begin{cases} \kappa_1 \cdot \bar{\kappa}_1^{n-1}, & n \in \mathbb{Z}^+, \kappa_1 \in (0, 1) \text{ if } i = 1 \\ \kappa_2 \cdot \bar{\kappa}_2^{n-1}, & n \in \mathbb{Z}^+, \kappa_2 \in (0, 1) \text{ if } i = 2. \end{cases}$$

Let N_n represent the number of data packets in the system at time $t = n^+$ and M_n represent the state of the system at time $t = n^+$. We define

$$M_n = \begin{cases} A, & \text{if the server is in busy state at time } t = n^+, \\ B, & \text{if the server is in type-I vacation state at time } t = n^+, \\ C, & \text{if the server is in type-II vacation state at time } t = n^+, \\ F, & \text{if the server is in failure state.} \end{cases}$$

It is observed that $\{N_n, M_n\}$ is a Markov chain with state space

$$\omega = \{(n, A), n = 0, 1, 2, \dots\} \cup \{(n, B), n = 0, 1, 2, \dots\} \cup \{(n, C), n = 0, 1, 2, \dots\} \cup F.$$

The one-step transition probabilities of $\{N_n, M_n\}$ is represented by

$$S_{(n_1, m_1), (n_2, m_2)} = P[X_{n+1} = (n_2, m_2) / X_n = (n_1, m_1)], n_1, n_2 \in N_n; m_1, m_2 \in M_n.$$

If $n_1 = n$ then $n_2 = n - 1$ or n or $n + 1$

State transitions and their corresponding transition parameters are presented in Table 1.

Table 1: State Transitions and its corresponding transition parameter

$S_{(n_1, m_1), (n_2, m_2)}$	Transition parameter
$S_{(n, A), (n+1, A)}$	$\begin{cases} \lambda \bar{\Psi} \bar{\zeta}, n = 0 \\ \lambda \bar{\mu} \bar{\zeta}, n = 1, 2, 3, \dots \end{cases}$
$S_{(n, A), (n-1, A)}$	$\bar{\lambda} \mu \bar{\zeta}, n = 1, 2, 3, \dots$
$S_{(n, B), (n+1, B)}$	$\begin{cases} \lambda \bar{\theta} \bar{\zeta}, n = 0 \\ \lambda \bar{\kappa}_1 \bar{\zeta}, n = 1, 2, 3, \dots \end{cases}$
$S_{(n, C), (n+1, C)}$	$\begin{cases} \lambda \bar{\zeta}, n = 0 \\ \lambda \bar{\kappa}_2 \bar{\zeta}, n = 1, 2, 3, \dots \end{cases}$
$S_{(n, A), (n, A)}$	$\begin{cases} \alpha_1, n = 0 \\ \alpha_5, n = 1, 2, 3, \dots \end{cases}$
$S_{(n, B), (n, B)}$	$\begin{cases} \alpha_2, n = 0 \\ \alpha_3, n = 1, 2, 3, \dots \end{cases}$
$S_{(n, C), (n, C)}$	$\begin{cases} \bar{\lambda}, n = 0 \\ \alpha_4, n = 1, 2, 3, \dots \end{cases}$
$S_{(0, A), (0, B)}$	$\Psi \bar{\lambda} \bar{\zeta}$
$S_{(0, B), (0, C)}$	$\theta \bar{\lambda} \bar{\zeta}$

$S_{(n_1, m_1), (n_2, m_2)}$	Transition parameters
$S_{(n, B), (n, A)}$	$\bar{\lambda}\kappa_1\bar{\zeta}, n = 1, 2, 3, \dots$
$S_{(n, C), (n, A)}$	$\bar{\lambda}\kappa_2\bar{\zeta}, n = 1, 2, 3, \dots$
$S_{(n, A), (F)}$	$\begin{cases} \beta_1, n = 0 \\ \beta_5, n = 1, 2, 3, \dots \end{cases}$
$S_{(n, B), (F)}$	$\begin{cases} \beta_2, n = 0 \\ \beta_3, n = 1, 2, 3, \dots \end{cases}$
$S_{(n, C), (F)}$	$\begin{cases} \zeta, n = 0 \\ \beta_4, n = 1, 2, 3, \dots \end{cases}$
$S_{(F), (0, A)}$	ω
$S_{(F, F)}$	$\bar{\omega}$

where

$$\begin{aligned} \beta_1 &= \lambda\Psi\zeta + \bar{\lambda}\Psi\zeta + \lambda\vartheta\zeta + \bar{\lambda}\vartheta\zeta, \beta_2 = \lambda\bar{\vartheta}\zeta + \bar{\lambda}\vartheta\zeta + \lambda\vartheta\zeta + \bar{\lambda}\bar{\vartheta}\zeta, \\ \beta_3 &= \lambda\bar{\kappa}_1\zeta + \bar{\lambda}\kappa_1\zeta + \lambda\kappa_1\zeta + \bar{\lambda}\bar{\kappa}_1\zeta, \beta_4 = \lambda\bar{\kappa}_2\zeta + \bar{\lambda}\kappa_2\zeta + \lambda\kappa_2\zeta + \bar{\lambda}\bar{\kappa}_2\zeta, \\ \beta_5 &= \lambda\bar{\mu}\zeta + \bar{\lambda}\mu\zeta + \lambda\mu\zeta + \bar{\lambda}\bar{\mu}\zeta, \alpha_1 = (\bar{\lambda}\bar{\Psi} + \lambda\Psi)\bar{\zeta}, \\ \alpha_2 &= (\bar{\lambda}\bar{\vartheta} + \lambda\vartheta)\bar{\zeta}, \alpha_3 = (\bar{\lambda}\bar{\kappa}_1 + \lambda\kappa_1)\bar{\zeta} \text{ and } \alpha_4 = (\bar{\lambda}\bar{\kappa}_2 + \lambda\kappa_2)\bar{\zeta}. \end{aligned}$$

The Kolmogorov equations for the investigated model are as follows:

$$\pi_F = (1 - \omega)\pi_F + \beta_1\pi_{0,A} + \beta_5\sum_{n=1}^{\infty}\pi_{n,A} + \beta_2\pi_{0,B} + \beta_3\sum_{n=1}^{\infty}\pi_{n,B} + \zeta\pi_{0,C} + \beta_4\sum_{n=1}^{\infty}\pi_{n,C}, \quad (1)$$

$$\pi_{0,A} = \alpha_1\pi_{0,A} + \omega\pi_F + \bar{\lambda}\mu\bar{\zeta}\pi_{1,A}, \quad (2)$$

$$\pi_{1,A} = \lambda\bar{\Psi}\bar{\zeta}\pi_{0,A} + \alpha_5\pi_{1,A} + \bar{\lambda}\mu\bar{\zeta}\pi_{2,A} + \bar{\lambda}\kappa_1\bar{\zeta}\pi_{1,B} + \bar{\lambda}\kappa_2\bar{\zeta}\pi_{1,C}, \quad (3)$$

$$\pi_{n,A} = \alpha_5\pi_{n,A} + \lambda\bar{\mu}\bar{\zeta}\pi_{n-1,A} + \bar{\lambda}\mu\bar{\zeta}\pi_{n+1,A} + \bar{\lambda}\kappa_1\bar{\zeta}\pi_{n,B} + \bar{\lambda}\kappa_2\bar{\zeta}\pi_{n,B}, n = 2, 3, 4, \dots, \quad (4)$$

$$\pi_{0,B} = \alpha_2\pi_{0,B} + \Psi\bar{\lambda}\bar{\zeta}\pi_{0,A}, \quad (5)$$

$$\pi_{1,B} = \alpha_3\pi_{1,B} + \lambda\bar{\vartheta}\bar{\zeta}\pi_{0,B}, \quad (6)$$

$$\pi_{n,B} = \alpha_3\pi_{n,B} + \lambda\bar{\kappa}_1\bar{\zeta}\pi_{n-1,B}, n = 2, 3, 4, \dots, \quad (7)$$

$$\pi_{0,C} = \bar{\lambda}\bar{\zeta}\pi_{0,C} + \vartheta\bar{\lambda}\bar{\zeta}\pi_{0,B}, \quad (8)$$

$$\pi_{1,C} = \alpha_4\pi_{1,C} + \lambda\bar{\zeta}\pi_{0,C}, \quad (9)$$

$$\pi_{n,C} = \alpha_4\pi_{n,C} + \lambda\bar{\kappa}_2\bar{\zeta}\pi_{n-1,C}, n = 2, 3, 4, \dots \quad (10)$$

3. STATIONARY ANALYSIS

The steady state probabilities of $\pi_{n,B}$, $\pi_{n,C}$, $\pi_{n,A}$ and π_F are presented in this section.

3.1. Evaluation of vacation state probabilities $\pi_{n,B}$ and $\pi_{n,C}$

Using Equations (5) – (7), we get

$$\pi_{n,B} = \begin{cases} \frac{\Psi\bar{\lambda}\bar{\zeta}}{1 - \alpha_2}\pi_{0,A}, & \text{if } n = 0, \\ \frac{\bar{\lambda}\bar{\lambda}\Psi\bar{\vartheta}\bar{\zeta}^2}{(1 - \alpha_2)(1 - \alpha_3)}\bar{\zeta}_1^{n-1}\pi_{0,A}, & \text{if } n = 1, 2, 3, \dots \end{cases} \quad (11)$$

Similarly, using Equations (8) – (10), we obtain

$$\pi_{n,C} = \begin{cases} \frac{\vartheta\Psi\bar{\lambda}^2\bar{\zeta}^2}{(1-\bar{\lambda}\bar{\zeta})(1-\alpha_2)}\pi_{0,A}, & \text{if } n = 0, \\ \frac{\lambda\bar{\lambda}^2\vartheta\Psi\bar{\zeta}^3}{(1-\bar{\lambda}\bar{\zeta})(1-\alpha_2)(1-\alpha_4)}\bar{\zeta}_2^{n-1}\pi_{0,A}, & \text{if } n = 1, 2, 3, \dots \end{cases} \quad (12)$$

where $\phi_1 = \frac{\lambda\bar{\kappa}_1\bar{\zeta}}{1-\alpha_3}$ and $\phi_2 = \frac{\lambda\bar{\kappa}_2\bar{\zeta}}{1-\alpha_4}$. Thus we have expressed the vacation state probabilities $\pi_{n,B}$ and $\pi_{n,C}$ in-terms of $\pi_{0,A}$. An explicit expression for $\pi_{0,A}$ is presented in Section 3.2.

3.2. Evaluation of $\pi_{n,A}$

The busy state probability $\pi_{n,A}$ is presented in this section. We define a generating function as follows:

$$H_z(n) = \sum_{n=1}^{\infty} \pi_{n,A}z^n.$$

Multiplying suitable powers of z on Equations (3) and (4), we get

$$\begin{aligned} \left\{ \lambda\bar{\mu}\bar{\zeta}z^2 - (1-\alpha_5)z + \bar{\lambda}\mu\bar{\zeta} \right\} H_z(n) &= \bar{\lambda}\mu\bar{\zeta}\pi_{1,A}z - \lambda\Psi\bar{\zeta}\pi_{0,A}z^2 - \bar{\lambda}\kappa_1\bar{\zeta}z \sum_{n=1}^{\infty} \pi_{n,B}z^n \\ &\quad - \bar{\lambda}\kappa_1\bar{\zeta}z \sum_{n=1}^{\infty} \pi_{n,C}z^n, \end{aligned}$$

where $\alpha_5 = (\bar{\lambda}\bar{\mu} + \lambda\mu)\bar{\zeta}$.

The above equation can be expressed as

$$\lambda\bar{\mu}\bar{\zeta}(z-\alpha)(z-\beta)H_z(n) = \bar{\lambda}\mu\bar{\zeta}\pi_{1,A}z - \lambda\Psi\bar{\zeta}\pi_{0,A}z^2 - \bar{\lambda}\kappa_1\bar{\zeta}z \sum_{n=1}^{\infty} \pi_{n,B}z^n - \bar{\lambda}\kappa_2\bar{\zeta}z \sum_{n=1}^{\infty} \pi_{n,C}z^n, \quad (13)$$

where

$$\alpha = \frac{(1-\alpha_5) + \sqrt{(1-\alpha_5)^2 - 4\lambda\bar{\lambda}\bar{\mu}\bar{\zeta}^2}}{2\lambda\bar{\mu}\bar{\zeta}},$$

and

$$\beta = \frac{(1-\alpha_5) - \sqrt{(1-\alpha_5)^2 - 4\lambda\bar{\lambda}\bar{\mu}\bar{\zeta}^2}}{2\lambda\bar{\mu}\bar{\zeta}}.$$

It is observed that $\beta < 1$ for any $0 < \lambda < 1$, $0 < \mu < 1$ and $0 < \zeta < 1$. Setting $z = \beta$ in Equation (13), we obtain

$$\bar{\lambda}\mu\bar{\zeta}\pi_{1,A} = \lambda\Psi\bar{\zeta}\pi_{0,A}\beta + \bar{\lambda}\kappa_1\bar{\zeta} \sum_{n=1}^{\infty} \pi_{n,B}\beta^n + \bar{\lambda}\kappa_2\bar{\zeta} \sum_{n=1}^{\infty} \pi_{n,C}\beta^n. \quad (14)$$

Applying Equation (14) in Equation (13), we get

$$\begin{aligned} H_z(n) &= \frac{\bar{\zeta}}{\bar{\mu}\alpha} \sum_{n=0}^{\infty} \left[\frac{1}{\alpha^n} + \frac{\lambda^2\kappa_1\Psi\bar{\vartheta}\bar{\zeta}}{(1-\alpha_2)(1-\alpha_3)(1-\beta\phi_1)} \sum_{k=0}^n \frac{\bar{\zeta}_1^{n-k}}{\alpha^k} + \frac{\lambda^3\kappa_2\Psi\vartheta\bar{\zeta}^2}{(1-\alpha_2)(1-\alpha_4)} \right. \\ &\quad \left. \times \frac{1}{(1-\bar{\lambda}\bar{\zeta})(1-\beta\phi_2)} \sum_{k=0}^n \frac{\bar{\zeta}_2^{n-k}}{\alpha^k} \right] z^{n+1}\pi_{0,A}. \end{aligned} \quad (15)$$

Comparing the coefficient of z^n on both sides of Equation (15), we obtain

$$\begin{aligned} \pi_{n,A} &= \frac{1}{\bar{\mu}\alpha^n} \left[\Psi + \frac{\bar{\lambda}^2\kappa_1\Psi\bar{\vartheta}\bar{\zeta}^2}{(1-\alpha_2)(1-\alpha_3)(1-\beta\phi_1)(\alpha\phi_1-1)} \{(\alpha\phi_1)^n - 1\} \right. \\ &\quad \left. + \frac{\bar{\lambda}^3\kappa_2\Psi\vartheta\bar{\zeta}^3}{(1-\alpha_2)(1-\alpha_4)(1-\bar{\lambda}\bar{\zeta})(1-\beta\phi_2)(\alpha\phi_2-1)} \{(\alpha\phi_2)^n - 1\} \right] \pi_{0,A}. \end{aligned} \quad (16)$$

The result (16) presents the explicit expression for the busy state probability in terms of $\pi_{0,A}$

3.3. Evaluation of Failure state probability π_F and $\pi_{0,A}$

The failure state probability π_F is obtained by using the results (11),(12) and (16) in Equation (1).

$$\begin{aligned} \pi_F = \frac{1}{\omega} & \left[\beta_1 + \frac{\beta_2 \Psi \bar{\lambda} \bar{\zeta}}{1 - \alpha_2} + \frac{\beta_5}{\bar{\mu}(\alpha - 1)} \left\{ 1 + \frac{\bar{\lambda}^2 \kappa_1 \Psi \bar{\theta} \bar{\zeta}^2}{(1 - \alpha_2)(1 - \alpha_3)(1 - \beta \phi_1)(1 - \phi_1)} \right. \right. \\ & + \left. \frac{\bar{\lambda}^3 \kappa_2 \Psi \bar{\theta} \bar{\zeta}^3}{(1 - \alpha_2)(1 - \alpha_4)(1 - \bar{\lambda} \bar{\zeta})(1 - \beta \phi_2)(1 - \phi_2)} \right\} + \frac{\zeta \bar{\theta} \Psi \bar{\lambda}^2 \bar{\zeta}^2}{(1 - \bar{\lambda} \bar{\zeta})(1 - \alpha_2)} \\ & \left. + \frac{\beta_3 \lambda \bar{\lambda} \Psi \bar{\theta} \bar{\zeta}^2}{(1 - \alpha_2)(1 - \alpha_3)(1 - \phi_1)} + \frac{\beta_4 \lambda \bar{\lambda}^2 \bar{\theta} \Psi \bar{\zeta}^3}{(1 - \bar{\lambda} \bar{\zeta})(1 - \alpha_2)(1 - \alpha_4)(1 - \phi_2)} \right] \pi_{0,A} \end{aligned} \quad (17)$$

An explicit expression for the idle state probability $\pi_{0,A}$ can be as follows: The normalisation condition for the investigated model is given by

$$\sum_{n=0}^{\infty} \pi_{n,A} + \sum_{n=0}^{\infty} \pi_{n,B} + \sum_{n=0}^{\infty} \pi_{n,C} + \pi_F = 1$$

Substituting the results (11), (12), (16) and (17) in the normalisation condition, we obtain

$$\pi_{0,A} = \frac{1}{D}, \quad (18)$$

where

$$\begin{aligned} D = & \left[\left(1 + \frac{\beta_1}{\omega} \right) + \left(1 + \frac{\beta_2}{\omega} \right) \frac{\Psi \bar{\lambda} \bar{\zeta}}{1 - \alpha_2} + \left(1 + \frac{\beta_3}{\omega} \right) \frac{\lambda \bar{\lambda} \Psi \bar{\theta} \bar{\zeta}^2}{(1 - \alpha_2)(1 - \alpha_3)(1 - \phi_1)} \right. \\ & + \left(1 + \frac{\zeta}{\omega} \right) \frac{\bar{\theta} \Psi \bar{\lambda}^2 \bar{\zeta}^2}{(1 - \bar{\lambda} \bar{\zeta})(1 - \alpha_2)} + \left(1 + \frac{\beta_4}{\omega} \right) \frac{\lambda \bar{\lambda}^2 \bar{\theta} \Psi \bar{\zeta}^3}{(1 - \bar{\lambda} \bar{\zeta})(1 - \alpha_2)(1 - \alpha_4)(1 - \phi_2)} \\ & + \left(1 + \frac{\beta_5}{\omega} \right) \frac{1}{\bar{\mu}(\alpha - 1)} \left\{ \bar{\Psi} + \frac{\bar{\lambda}^2 \kappa_1 \Psi \bar{\theta} \bar{\zeta}^2}{(1 - \alpha_2)(1 - \alpha_3)(1 - \beta \phi_1)(1 - \phi_1)} \right. \\ & \left. \left. + \frac{\bar{\lambda}^3 \kappa_2 \Psi \bar{\theta} \bar{\zeta}^3}{(1 - \alpha_2)(1 - \alpha_4)(1 - \bar{\lambda} \bar{\zeta})(1 - \beta \phi_2)(1 - \phi_2)} \right\} \right]. \end{aligned}$$

Remark It is noted that if $\zeta = 0$ and $\Psi = 0$ then the result (16) reduces to

$$\pi_{n,A} = \frac{1}{1 - \mu} \left\{ \frac{\lambda}{\mu} \left(\frac{1 - \mu}{1 - \lambda} \right) \right\}^n \pi_{0,A}$$

where

$$\pi_{0,A} = 1 - \frac{\lambda}{\mu}$$

The above expression coincides with Equation (24) of Taha [17]

4. PERFORMANCE MEASURES

This section presents the performance measures of the investigated system

4.1. Expected system size

Let $E(N_{DP})$ denote the expected number of data packets in the system, then

$$\begin{aligned}
 E(N_{DP}) &= \sum_{n=1}^{\infty} n (\pi_{n,A} + \pi_{n,B} + \pi_{n,C}) \\
 &= \frac{1}{\bar{\mu}} \left[\frac{\Psi\alpha}{(\alpha-1)^2} + \frac{\bar{\lambda}^2\kappa_1\Psi\bar{\vartheta}\bar{\zeta}^2}{(1-\alpha_2)(1-\alpha_3)(1-\beta\phi_1)(\alpha\phi_1-1)} \left\{ \frac{\phi_1}{(1-\phi_1)^2} - \frac{\alpha}{(\alpha-1)^2} \right\} \right. \\
 &\quad + \frac{\bar{\lambda}^3\kappa_2\Psi\bar{\vartheta}\bar{\zeta}^3}{(1-\alpha_2)(1-\alpha_4)(1-\bar{\lambda}\bar{\zeta})(1-\beta\phi_2)(\alpha\phi_2-1)} \left\{ \frac{\phi_2}{(1-\phi_2)^2} - \frac{\alpha}{(\alpha-1)^2} \right\} \\
 &\quad \left. + \frac{\lambda\bar{\lambda}\Psi\bar{\vartheta}\bar{\zeta}^2}{(1-\alpha_2)(1-\alpha_3)(1-\bar{\zeta}_1)^2} + \frac{\lambda\bar{\lambda}^2\vartheta\Psi\bar{\zeta}^3}{(1-\bar{\lambda}\bar{\zeta})(1-\alpha_2)(1-\alpha_4)(1-\bar{\zeta}_2)^2} \right] \pi_{0,A}.
 \end{aligned}$$

4.2. Probability that the server is in vacation state

Let $\pi_{\bullet,B}$ and $\pi_{\bullet,C}$ denote the probability that the server is in short and long vacation respectively. Then

$$\pi_{\bullet,i} = \sum_{n=0}^{\infty} \pi_{n,i} = \begin{cases} \frac{\Psi\bar{\lambda}\bar{\zeta}}{1-\alpha_2} \left[1 + \frac{\lambda\bar{\vartheta}\bar{\zeta}}{(1-\alpha_3)(1-\bar{\zeta}_1)} \right] \pi_{0,A}, & \text{if } i = B \\ \frac{\vartheta\Psi\bar{\lambda}^2\bar{\zeta}^2}{(1-\bar{\lambda}\bar{\zeta})(1-\alpha_2)} \left[1 + \frac{\lambda^2\bar{\zeta}}{(1-\alpha_4)(1-\bar{\zeta}_2)} \right] \pi_{0,A}, & \text{if } i = C \end{cases}$$

4.3. Probability that the server is in busy

Let $\pi_{\bullet,A}$ denote the probability that the server is busy, then

$$\begin{aligned}
 \pi_{\bullet,A} &= \sum_{n=1}^{\infty} \pi_{n,A} \\
 &= \frac{1}{\bar{\mu}(\alpha-1)} \left[\Psi + \frac{\bar{\lambda}^2\kappa_1\Psi\bar{\vartheta}\bar{\zeta}^2}{(1-\alpha_2)(1-\alpha_3)(1-\beta\phi_1)(1-\phi_1)} + \frac{\bar{\lambda}^3\kappa_2\Psi\bar{\vartheta}\bar{\zeta}^3}{(1-\alpha_2)(1-\alpha_4)(1-\bar{\lambda}\bar{\zeta})} \right. \\
 &\quad \left. \times \frac{1}{(1-\beta\phi_2)(1-\phi_2)} \right] \pi_{0,A}
 \end{aligned}$$

The expression for $\pi_{0,A}$ is presented in the result (18).

5. NUMERICAL ILLUSTRATION

This section presents the numerical illustration for the investigated model. The values of the parameter as choose as follows: $\lambda = 0.3$, $\mu = 0.7$, $\psi = 0.2$, $\vartheta = 0.2$, $\zeta = 0.01$, $\omega = 0.4$, $\kappa_1 = 0.2$ and $\kappa_2 = 0.4$. Figure 2 presents the behaviour of $\pi_{n,B}$ for various arrival rates λ . The graph shows that as λ increases, the probability $\pi_{n,B}$ decreases, indicating that higher arrival rates result in lower probabilities of having more packets in the system during the T_{V_1} period.

Figure 3 displays the probability curves of $\pi_{n,B}$ for different values of κ_1 . It is evident that as κ_1 increases, the probability $\pi_{n,B}$ for $n = 0$ rises slightly, indicating a higher likelihood of an empty system when the server switches more frequently from the vacation to the busy state. This suggests that with faster switching, the system is cleared more efficiently, reducing the chance of data packets accumulating during the serverTMs vacation period. On the other hand, for $n = 1$ to $n = 10$, the values of $\pi_{n,B}$ consistently decrease as κ_1 increases. This trend indicates that when the server switches back to the busy state more frequently, the system spends less time in the

vacation state with non-zero packets. Consequently, the probability of data packets in the system during the vacation state decreases with increasing κ_1 .

In Figure 4, we can see the behaviour of the T_{V_2} state for different arrival rates λ . As the arrival rate λ increases, the probability $\pi_{n,C}$ generally decreases when $n = 0$, indicating that the chance of having an empty system is lower at higher arrival rates. As the value of n increases, the values of $\pi_{n,C}$ consistently decrease across all λ values. This suggests that as the arrival rate increases, the likelihood of having a larger number of packets in the vacation state becomes smaller.

In Figure 5, the probability curves of $\pi_{n,C}$ are shown for different values of κ_2 . As κ_2 increases, the probabilities $\pi_{n,C}$ decrease for higher values of n , indicating that a higher switching rate reduces the likelihood of a large number of packets building up in the system. This is because as κ_2 increases, the server switches from vacation to busy mode more quickly, processing data packets more frequently and reducing congestion during the vacation state. For smaller values of n , such as $n = 0, 1, 2$, the differences between the probabilities for different κ_2 values are less noticeable. However, as n increases, particularly beyond $n = 4$, the impact of a higher κ_2 becomes more apparent, with a more pronounced decline in $\pi_{n,C}$.

In Figure 6, we can see how the busy state $\pi_{n,A}$ behaves for different values of λ . When $n = 0$, the probability $\pi_{0,A}$ decreases as λ increases, indicating that a higher arrival rate makes it less likely for the system to be idle. As n increases, the probabilities $\pi_{n,A}$ generally decrease for larger n , meaning it becomes less likely for many packets to accumulate in the system. However, for intermediate values of n , like $n = 1$ and $n = 2$, the probabilities slightly increase with higher λ , suggesting that more packets are expected in the system when the arrival rate is higher. Overall, the behaviour of $\pi_{n,A}$ across different λ values indicates that higher arrival rates increase the likelihood of having more data packets in the system during the busy state.

Figure 7 shows the probability curves of the busy state $\pi_{n,A}$ for various values of μ . Observing the probabilities, we see that for $n = 0$, $\pi_{0,A}$ increases as μ increases. This trend suggests that a higher service rate leads to a higher probability of the system being idle, likely because packets are processed more quickly, reducing the chance of any being present in the busy state. For values of n greater than 0, the probability $\pi_{n,A}$ generally decreases as μ increases. This indicates that higher service rates effectively reduce the likelihood of the system having many packets, as the server can handle incoming traffic more efficiently.

Figure 8 presents the probability of having n packets in the busy state $\pi_{n,A}$ for various values of κ_1 . As the rate κ_1 increases, the probability $\pi_{n,A}$ of having n data packets in the busy state shows a clear pattern. For $n = 0$ and $n = 1$, $\pi_{n,A}$ increases, meaning the system is more likely to have fewer packets as the server switches faster. For instance, $\pi_{0,A}$ rises as κ_1 increases from 0.1 to 0.4. However, for larger n , $\pi_{n,A}$ decreases with higher κ_1 , indicating that faster switching reduces the likelihood of accumulating more packets in the busy state. This reflects the server's improved efficiency in managing data packets.

Figure 9 presents the behaviour $\pi_{n,A}$ for various values of κ_2 . It is observed that $\pi_{n,A}$ decreases as n increases, indicating that the probability of having a higher number of packets in the system diminishes as n increases. Additionally, as κ_2 increases, the probabilities for smaller values of n rise, signifying that when the server switches more quickly from the vacation state to the busy state, the system is more likely to have fewer packets. Conversely, for larger values of n , such as $n = 10$, the probability decreases more rapidly for higher κ_2 . This trend highlights the role of κ_2 in maintaining system stability, as higher switching rates lead to lower probabilities of larger packet queues, suggesting that the system is more stable with fewer packets when the server can quickly switch from vacation to the busy state.

Figure 10 displays the mean system size $E(N_s)$, which represents the average number of data packets in the system, for different values of the arrival rate λ and the disaster rate ζ . From the figure, we observe that the mean system size increases as λ increases, regardless of the disaster rate ζ . This indicates that higher arrival rates of packets lead to larger system sizes, which is expected as more packets are entering the system. Additionally, for each value of λ , increasing ζ results in a smaller system size, reflecting the effect of more frequent disasters clearing the system.

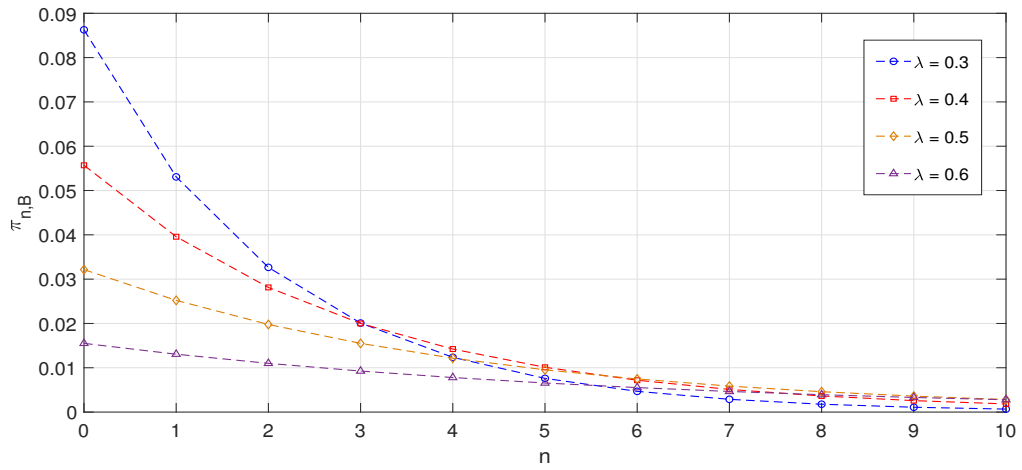


Figure 2: Probabilities of the type-I vacation $\pi_{n,B}$ for different values of λ .

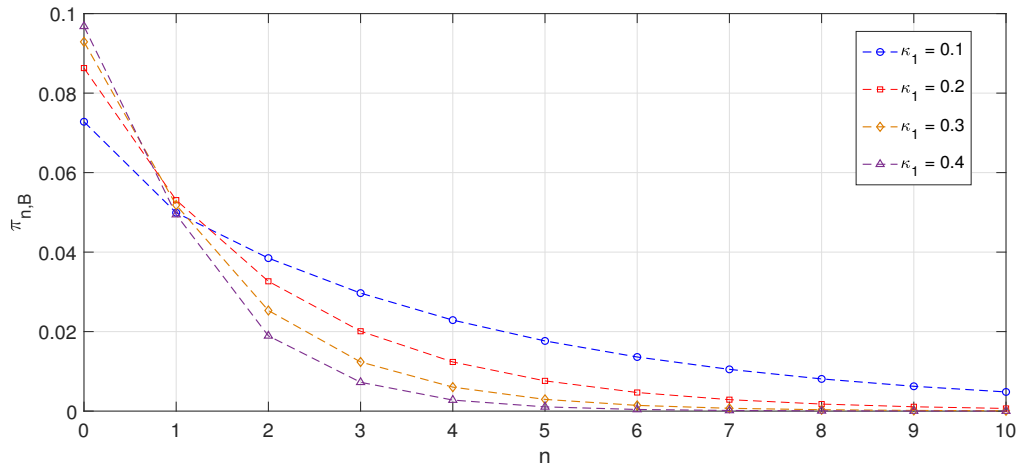


Figure 3: Probabilities of the type-I vacation $\pi_{n,B}$ for different values of κ_1 .

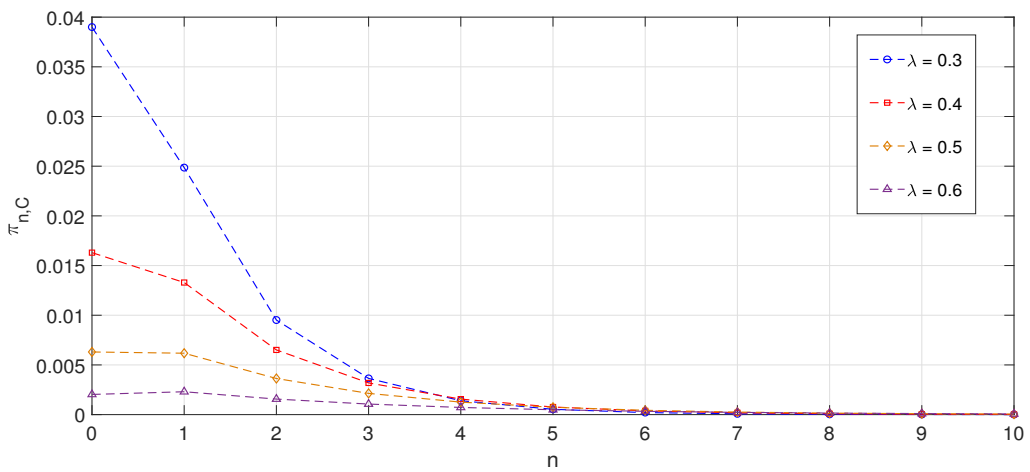


Figure 4: Probabilities of the type-II vacation $\pi_{n,C}$ for different values of λ .

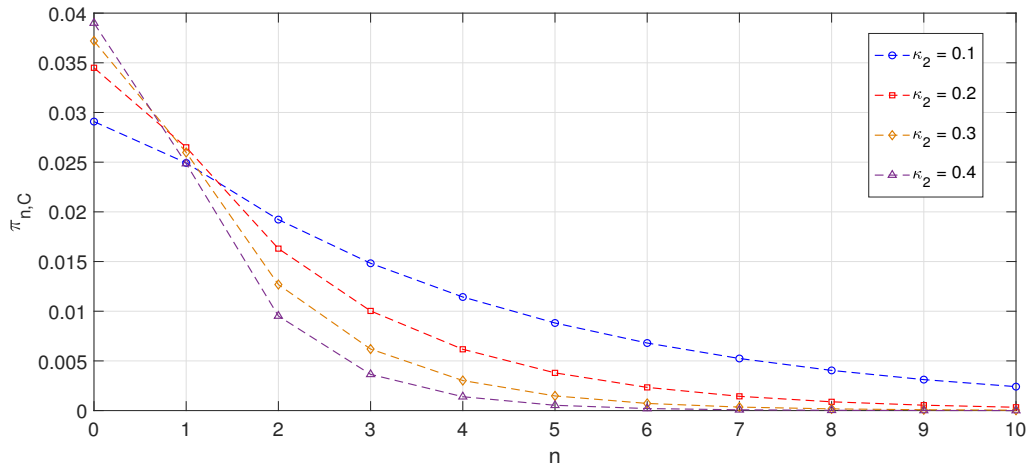


Figure 5: Probabilities of the type-II vacation $\pi_{n,C}$ for different values of κ_2 .

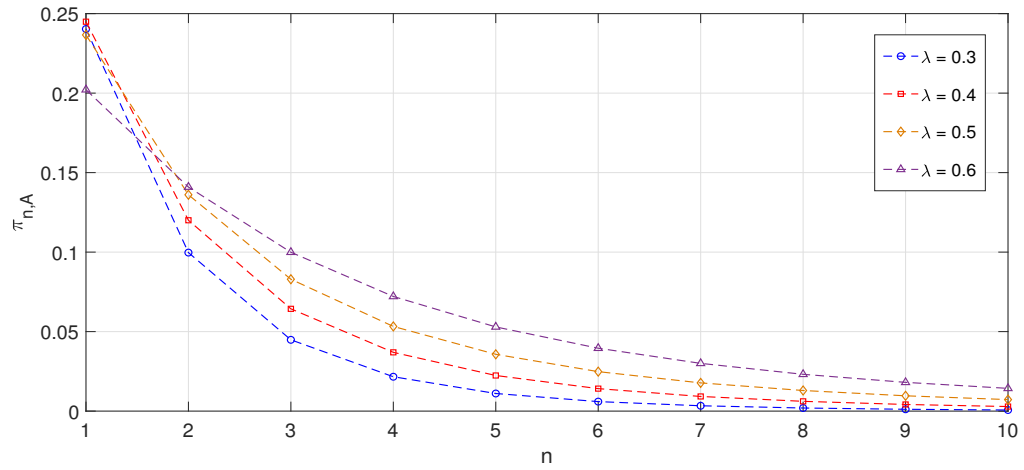


Figure 6: Probabilities of the busy state $\pi_{n,A}$ for different values of λ .

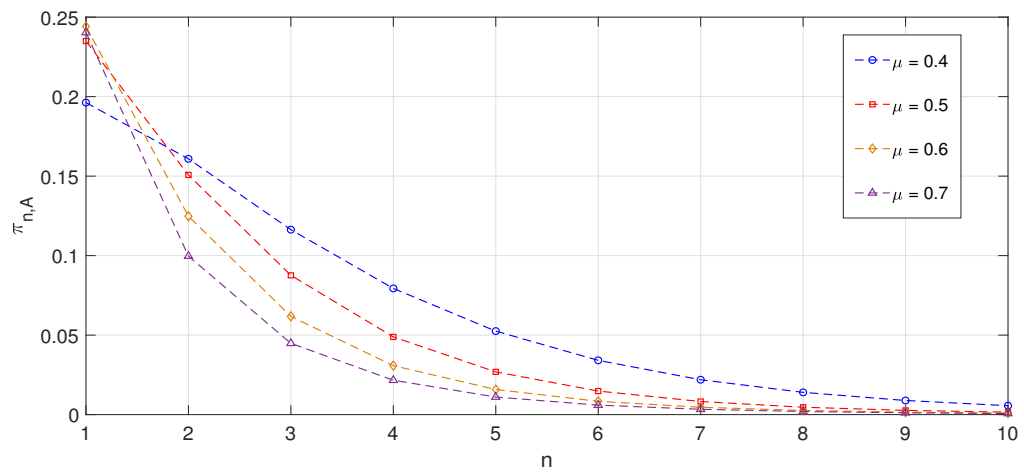


Figure 7: Probabilities of the busy state $\pi_{n,A}$ for different values of μ .

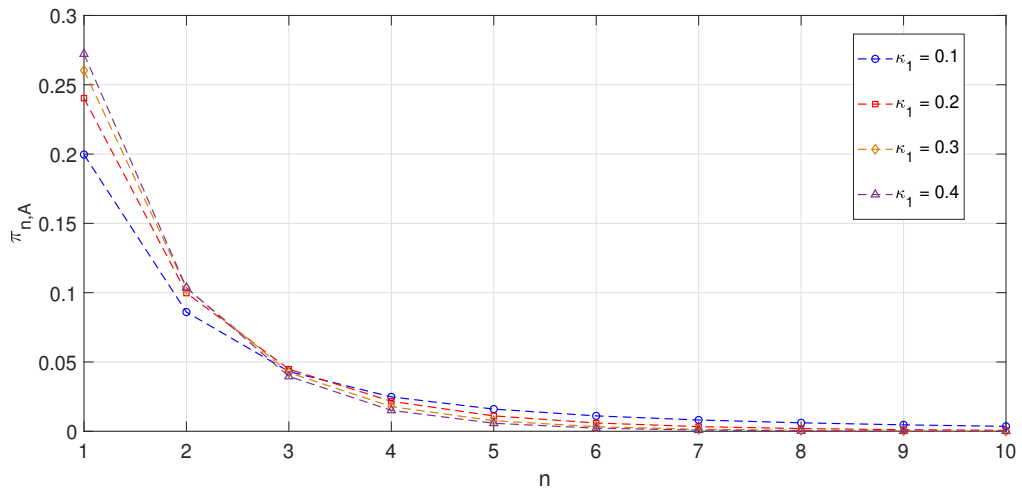


Figure 8: Probabilities of the busy state $\pi_{n,A}$ for different values of κ_1 .

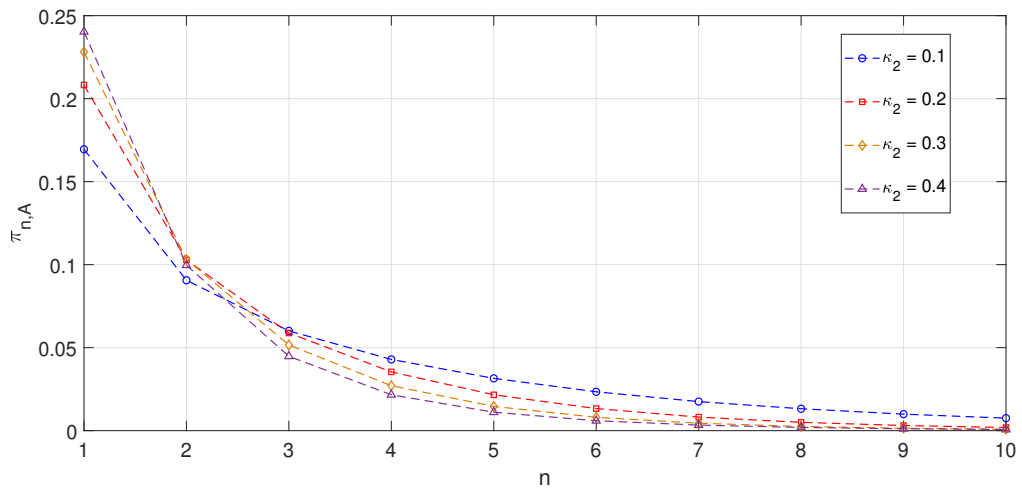


Figure 9: Probabilities of the busy state $\pi_{n,A}$ for different values of κ_2 .

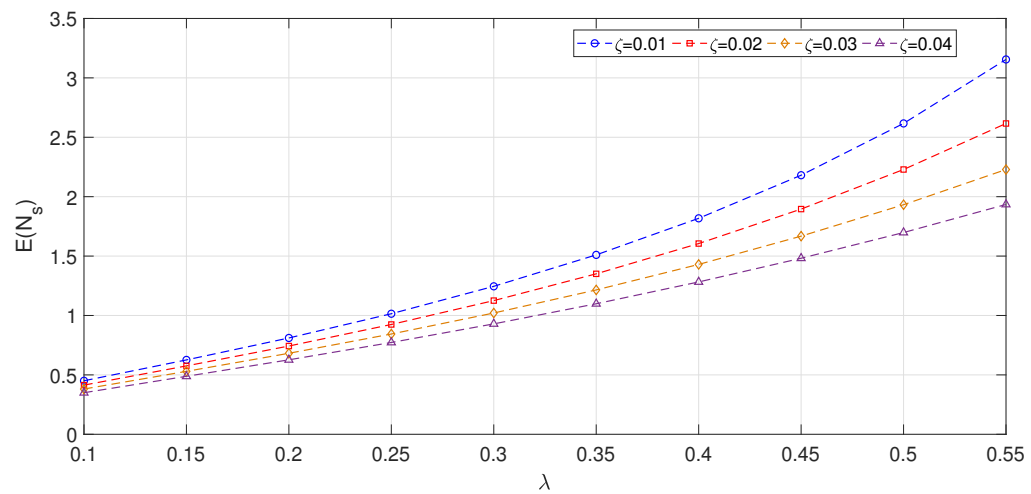


Figure 10: Expected system size for different values of ζ .

6. CONCLUSION

This paper analyzed the DRX mechanism, a critical power-saving feature in wireless communication systems, using a discrete-time Geo/Geo/1 queueing model with DV policy and disaster. By incorporating the DV policy, we captured the varying duration of sleep periods, providing a more granular and realistic evaluation of DRX performance compared to traditional continuous-time models. Our findings demonstrate that the DRX mechanism, when modelled through differentiated vacations, can effectively balance energy efficiency and network performance. The current study focused on a single server setup. One can extend this work by investigating multi-server configurations.

REFERENCES

- [1] Ayman E (2014) Extending the battery life of smartphones and tablets: a practical approach to optimizing the lte network. *IEEE Veh Technol Mag* 9(2):38-49.
- [2] Di Crescenzo, A., Giorno, V., Nobile, A. G., & Ricciardi, L. M. (2003). On the M/M/1 queue with catastrophes and its continuous approximation. *Queueing Systems*, 43, 329-347.
- [3] Dimitriou, I. (2016). Queueing analysis of the DRX power saving mechanism in fault-tolerant 3GPP LTE wireless networks. *Annals of Operations Research*, 239(2), 521-552.
- [4] De Turck, K., De Vuyst, S., Fiems, D., Wittevrongel, S., & Bruneel, H. (2012). Performance analysis of sleep mode mechanisms in the presence of bidirectional traffic. *Computer Networks*, 56, 2494-2505.
- [5] Ibe, O. C., & Isijola, O. A. (2014). M/M/1 multiple vacation queueing systems with differentiated vacations. *Modelling and Simulation in Engineering*, 2014(1), 158247.
- [6] Jain, G., & Sigman, K. (1996). A Pollaczek-Khintchine formula for M/G/1 queues with disasters. *Journal of Applied Probability*, 33(4), 1191-1200.
- [7] Kalita, P., & Selvamuthu, D. (2023). Stochastic modelling of sleeping strategy in 5G base station for energy efficiency. *Telecommunication Systems*, 83(2), 115-133.
- [8] Kumar, A., Kaswan, S., Devanda, M., & Shekhar, C. (2023). Transient analysis of queueing-based congestion with differentiated vacations and customerTMs impatience attributes. *Arabian Journal for Science and Engineering*, 48(11), 15655-15665.
- [9] Lee, D. H., & Yang, W. S. (2013). The N-policy of a discrete time Geo/G/1 queue with disasters and its application to wireless sensor networks. *Applied Mathematical Modelling*, 37(23), 9722-9731.
- [10] Mittal, N., Jain, V., & Dharmaraja, S. (2023). Power efficient stochastic modeling for Narrow-band Internet of Things devices in 5G networks. *Transactions on Emerging Telecommunications Technologies*, 34(9), e4825.
- [11] Mohammed Shapique, A., Sudhesh, R., & Dharmaraja, S. (2024). Transient Analysis of a Modified Differentiated Vacation Queueing System for Energy-Saving in WiMAX. *Methodology and Computing in Applied Probability*, 26(3), 23.
- [12] Raj, R., & Dharmaraja, S. (2023). Stochastic modelling of multi-layer HAP-LEO systems in 6G for energy saving: An analytical approach. *Computer Communications*, 210, 22-34.
- [13] Suranga Sampath, M. I. G., & Liu, J. (2020). Impact of customersTM impatience on an M/M/1 queueing system subject to differentiated vacations with a waiting server. *Quality Technology & Quantitative Management*, 17(2), 125-148.
- [14] Sudhesh, R., & Mohammed Shapique, A. (2022). Transient analysis of power management in wireless sensor network with start-up times and threshold policy. *Telecommunication Systems*, 80(1), 1-16.
- [15] Sudhesh, R., & Vaithyanathan, A. (2021). Stationary analysis of infinite queueing system with two-stage network server. *RAIRO-Operations Research*, 55, S2349-S2357.
- [16] Sudhesh, R., Mohammed shapique, A., & Dharmaraja, S. (2022). Analysis of a multiple dual-stage vacation queueing system with disaster and repairable server. *Methodology and Computing in Applied Probability*, 24(4), 2485-2508.

- [17] El-Taha, M. (2023). A Review of Birth?Death and Other Markovian Discrete?Time Queues. *Advances in Operations Research*, 2023(1), 6620393.
- [18] Vijayashree, K. V., & Janani, B. (2018). Transient analysis of an M/M/1 queueing system subject to differentiated vacations. *Quality Technology & Quantitative Management*, 15(6), 730-748.
- [19] Yang, S.-R., & Lin, Y.-B. (2005). Modeling UMTS discontinuous reception mechanism. *IEEE Transactions on Wireless Communications*, 4(1), 312–319.
- [20] Yang, S.-R., Yan, S., & Hung, H. (2007). Modeling UMTS power saving with bursty packet data traffic. *IEEE Transactions on Mobile Computing*, 6(12), 1398–1409.
- [21] 3GPP TS 36.321, Evolved Universal Terrestrial Radio Access (EUTRA); Medium Access Control (MAC) protocol specification (version 9.3.0 Release 9), 2010.